

Fault Diagnostics in Shipboard Power Systems using Graph Neural Networks

Roshni Anna Jacob, *Student Member, IEEE*, Soroush Senemmar, *Student Member, IEEE*,
and Jie Zhang, *Senior Member, IEEE*

The University of Texas at Dallas
Richardson, TX 75080, USA

Email: {roshni.jacob, soroush.senemmar, jiezhang}@utdallas.edu

Abstract—Shipboard power systems are evolving into sophisticated networks with automated protection and predictive control infrastructure. The need for real-time fault monitoring and detection in such systems can be facilitated by employing deep learning techniques. Taking into consideration the characteristic graph nature of the power network, this paper solves the fault detection and classification problem using graph convolutional neural networks. The proposed methodology translates the dynamic voltage measurements at the busbars of a shipboard power network along with the topology into input features for the learning framework. Both the type of fault and the location of the fault are determined. The developed model is validated on an 8-bus shipboard test network. The results indicate that the proposed algorithm has superior performance and can detect the fault type and location with an above 99% accuracy.

Index Terms—Graph convolution network, fault detection, shipboard power system

I. INTRODUCTION

The future generation of ships are moving towards unmanned surface vessels, which are more sophisticated, economically efficient, and eco-friendly [1], [2]. Besides this, modern Navy ships have been undergoing rapid growth in both size and complexity, which may lead to increased malfunctions and challenges in energy management. For instance, Navy shipboard power systems (SPS) will consist of new emerging technologies such as the integrated power system, pulsed power loads, energy storage, and others [3]. Therefore, it is essential to manage the SPS automatically by including predictive maintenance and corrective actions even when there is no one on board to address it.

Meanwhile, one of the most important actions in future navy ships is SPS protection, which is defined as fault detection, classification (e.g., single phase to ground, line to line, and three phase), and location identification in the SPS. SPS protection methods include traditional methods such as distance protection, overcurrent protection, current differential protection, and intelligent methods such as wavelet analysis and artificial neural based networks. Recently, the application of machine/deep learning to fault detection in power systems has

significantly increased due to its benefits. The machine/deep learning-based methods can detect the faults more accurately [4] and faster compared to traditional methods [5]. Accurate fault detection and classification enables proper isolation of faults, while the fast speed in determining the fault location can significantly reduce the maintenance time, and improve the post-fault system reconfiguration, and thereby the system reliability.

Fault diagnosis has been performed using machine/deep learning techniques in recent works. For example, support vector machine (SVM) was used for fault detection and classification in transmission networks [6], where dynamic busbar voltages were used to detect and classify the fault type with an accuracy of more than 93%. The steady state voltage measurements at the busbars of an IEEE 37-bus network were used to detect the fault, classify the fault type, and determine the fault location in [7] using artificial neural network (ANN). Yu et al. [4] developed a recurrent neural network (RNN) based method, specifically using the gated recurrent units (GRU), to detect and classify the fault in a microgrid, with an over 97% accuracy.

Recently, deep learning based methods have also been used for fault detection in SPS [7]–[11]. For instance, in [7], the fault type in medium voltage DC (MVDC) SPS is determined using a fully connected deep neural network (DNN) with an accuracy of more than 95%. Ma et al. [8] adopted long short-term memory (LSTM) for DC load monitoring and detecting component faults through the time-series current signals of the DC-pulsed load. In [9], the authors used an ANN for fault detection and classification in MVDC SPS with a 99% accuracy for classifying fault types at each busbar.

Most of these learning frameworks utilize data in the Euclidean domain to categorize the faults. However, in such tasks, the measurements derived from a power network are essentially data superimposed on an underlying graph and therefore can be characterized as non-Euclidean. Over the recent years, several deep learning methods for graph-based data have been developed. Two approaches for convolution on graph neural networks (GNN) are spectral [12], [13], [14] and spatial [15], [16], [17]. Spatial techniques use information propagation along the edges and spectral techniques rely on the graph spectral theory to perform convolution on the graphs

This work relates to Department of Navy award (N00014-20-1-2795) issued by the Office of Naval Research. The United States Government has a royalty-free license throughout the world in all copyrightable material contained herein.

given the node and edge data. The graph convolution network (GCN) proposed in [14] is rooted in graph signal processing with a spectral-based approach for convolution. Additionally, in [14], the spatial features of the nodes are also incorporated into the learning framework by aggregating neighborhood nodal information for each node under consideration. Recognizing the potential of GNN in graph specific problems, a few power system applications have employed GNN for learning tasks such as power flow estimation [18], load shedding [19], output power prediction [20] and fault diagnosis [21].

In the proposed work, fault diagnostics is performed for an SPS as opposed to the radial distribution network as in [21]. Most of the authors have used steady state or quasi-static time series measurements for fault classification. However, in the proposed approach, the dynamic modeling and electromagnetic transient (EMT) capabilities of DigSILENT have been exploited to derive the voltage measurements at various buses, resulting in an accurate description of system behavior during faults. Additionally, identification of the fault type is also learned in the developed model.

The contributions of this work include (i) developing a GCN-based deep learning architecture to detect and classify the location and type of faults in shipboard power networks, and (ii) enabling real-time monitoring of faults using the developed model by learning the signature dynamic patterns from busbar voltages. The rest of the paper is organized as follows. The SPS fault detection problem is formulated in section II. Section III discusses the proposed GCN-based deep learning approach used for fault detection and identification. The simulation results of an 8-bus SPS are presented and discussed in section IV. Finally, the conclusions are given in Section V.

II. PROBLEM DESCRIPTION

Figure 1 shows a synthetic shipboard power system (SPS), which is a standard 3-phase MVAC 8-bus SPS, working under the 13.8 kV voltage and 50 Hz frequency [22]. Busbar 1 (BB1) is considered as the reference busbar in the SPS. There are two main generators (G1 and G3) and two auxiliary generators (G2 and G4) in the SPS to meet the loads. There are six load points numbered 1 to 6 where all the loads at each zone are aggregated in one of the loads. The network cable characteristics are modeled based on MVAC distribution cables. The two main generators have the rated power of 36 MW with a 0.9 power factor (PF). The two auxiliary generators have the rated power of 4 MW with a 0.8 PF. The rated voltage of generators is 13.8 kV. The voltage control mode for G1 is based on the voltage, and for other generators is based on PF. Each of the L2 and L5 nodes has 30 MW load with a 0.9 PF; each of the L1, L3, L4, and L6 nodes has 2 MW load with a 0.9 PF. In [23], we have used deep learning models such as LSTM, GRU for fault diagnostics on the 8-bus shipboard power system. The test system and the dynamic voltage profiles as that in [23] are used in this paper. However, the topological features and nodal interdependency which were

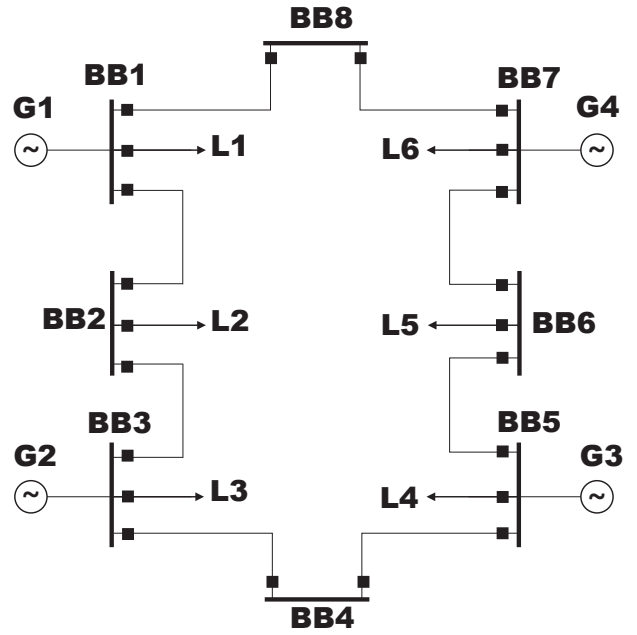


Fig. 1: An 8-bus shipboard power system [23]

not factored in [23] are considered by using the graph neural network in this paper.

A. Power flow simulations and fault scenarios

The proposed SPS model in Fig. 1 is simulated in the DIgSILENT PowerFactory software [24], to generate and simulate different fault scenarios. In this model, three busbars of BB1, BB4, and BB6, are considered for fault simulation scenarios. At each busbar, three types of faults are simulated, including single-line to ground (LG), line-to-line (LL), and three-phase (3L) faults. In each simulation, a 5-second time frame is considered in which at second 0.5 the fault occurs. Voltages of all busbars are sampled during this time frame with 200 samples per voltage cycle. The simulations are conducted based on time-series EMT simulations in the software.

B. Fault simulations and data sampling

As earlier mentioned, the time-frame for simulations is 5 seconds. Therefore, there are 50,000 samples per line voltage and each busbar has three line voltage (AB, BC, and AC); thus the vector of sampled data is $50,000 \times 24$, where the rows represent sample-steps and columns represent line voltages of all busbars. Figures 2-4 show the sampled voltages of all busbars when the LG fault (Fig. 2), LL fault (Fig. 3), or 3L fault (Fig. 4) occurs on BB1. It can be seen that the voltages are in normal operation before second 0.5 (i.e. when the fault occurs), and begin to decrease after the fault. Hence, the data extracted from the voltage profile contains both fault-free and faulty modes.

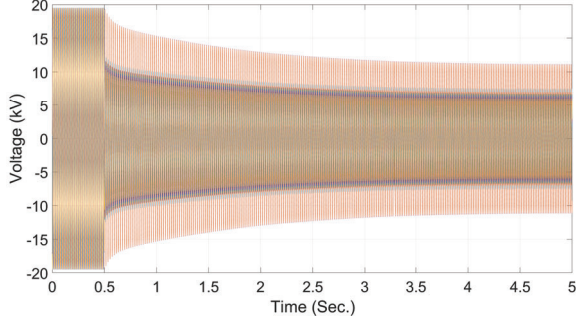


Fig. 2: Busbar voltages with LG fault on BB1 [23].

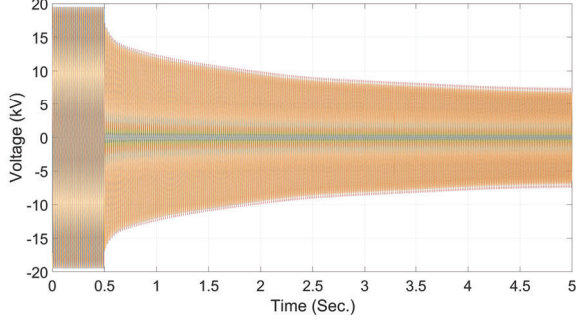


Fig. 3: Busbar voltages with LL fault on BB1 [23].

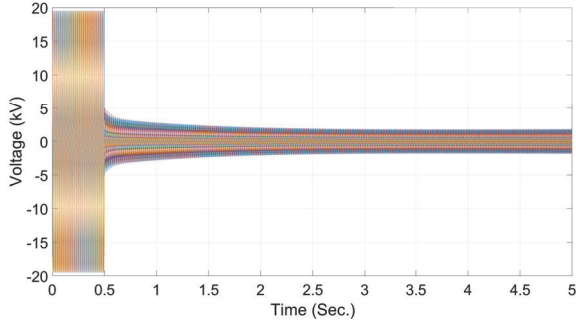


Fig. 4: Busbar voltages with 3L fault on BB1 [23].

III. LEARNING USING GRAPH CONVOLUTIONAL NEURAL NETWORKS

A. Graph convolution

Featured graphs are composed of both structural and spectral data. Latent representations can be drawn from the spatial and spectral information encompassed in the nodes using GCN. The convolution performed on graphs in GCN is based on graph signal processing and spectral theory. Consider an undirected graph represented as $\mathcal{G} = (N, E)$, where N is the set of nodes and E is the set of edges. The topology of the graph is described by the adjacency matrix A . Using the degree matrix of the graph where the entries are calculated by $D_{ii} = \sum_{j=1}^n A_{ij}$; $\forall i \in N$, the normalized graph Laplacian is estimated using:

$$L_G = I - D^{-\frac{1}{2}} A D^{-\frac{1}{2}} \quad (1)$$

The eigendecomposition of the positive semidefinite matrix $L_G = \Theta \Lambda \Theta^T$.

The node features of the graph are represented using a matrix X of dimensions (n, f) , where n is the number of graph nodes and f is the number of features extracted for each node. Each feature is considered as a signal on the node and hence a graph signal is represented as $\mathbf{x} \in \mathbb{R}^n$. Further, the graph Fourier transform on \mathbf{x} is $\mathcal{F}(\mathbf{x}) = \Theta^T \mathbf{x}$, and its inverse is $\mathcal{F}^{-1}(\tilde{\mathbf{x}}) = \Theta \tilde{\mathbf{x}}$. As a result, the graph convolution of the graph signal \mathbf{x} with a filter \mathbf{U} is:

$$\begin{aligned} \mathbf{x} *_g \mathbf{U} &= \mathcal{F}^{-1}(\mathcal{F}(\mathbf{x}) \circ \mathcal{F}(\mathbf{U})) \\ &= \Theta(\Theta^T \mathbf{x} \circ \Theta^T \mathbf{U}) \end{aligned} \quad (2)$$

Performing the element wise multiplication ‘ \circ ’ on the filter $\mathbf{U} = \text{diag}(\Theta^T \mathbf{u})$, the resulting expression for graph signal convolution is:

$$\mathbf{x} *_g \mathbf{U} = \Theta \mathbf{U} \Theta^T \mathbf{x} \quad (3)$$

In [13], a chebyshev polynomial of the diagonal matrix of eigenvalues of the normalized graph Laplacian, L_G , is used for filtering the graph signal. With the eigenvector as λ , the diagonal matrix of eigenvalues as $\Lambda = \text{diag}(e_0, e_1, e_2, \dots, e_{n-1})$, and $\tilde{\lambda} = 2\lambda / \max(e_0, e_1, \dots, e_{n-1}) - I$, the chebyshev polynomial is represented as $H_k(\tilde{\lambda})$. The resulting graph convolution is then given by:

$$\mathbf{x} *_g \mathbf{U} = \sum_{k=0}^K \alpha_k H_k(\tilde{\lambda}) \mathbf{x} \quad (4)$$

A first order approximation of the Chebyshev filter is used in [14]. Therefore with $K = 1$, $\alpha_0 = -\alpha_1 = \alpha$, and $\max(e_0, e_1, \dots, e_{n-1}) = 2$, the convolution on the graph signal is expressed as:

$$\mathbf{x} *_g \mathbf{U} = \alpha(I + D^{-\frac{1}{2}} A D^{-\frac{1}{2}}) \mathbf{x} \quad (5)$$

The GCN layer in the developed learning model uses the specified graph convolution operation on the feature signals.

B. Network architecture

The main component of the learning network is the GCN layer which extracts latent representations from the network topology and node information signals. The input to the learning architecture is the matrix comprising of features of all the nodes, X , and the adjacency matrix A . Two different architectures are used for determining the location and type of fault. In both these graph learning networks, following the input layer, three GCN layers with a filter size of 32 each are used to derive the hidden network representations. Suitable activation functions are selected for the layers based on the model performance during experimentation.

Eq. (5) can be extended to the case with multiple input and output channels, therefore the output of GCN layer is represented as:

$$\hat{Y} = X *_g \mathbf{U} = \sigma(\bar{A} X \mathbf{W}) \quad (6)$$

where \hat{Y} is the matrix of convolved signals, W is the filter parameter matrix, and σ is the activation function. The adjacency matrix A is modified to \bar{A} using:

$$\bar{A} = I + D^{-\frac{1}{2}} A D^{-\frac{1}{2}} \quad (7)$$

The output of the last GCN layer is pooled and given to a dense layer with 512 units. An additional dense layer with 256 units is used in the learning network for the classification of fault type. The softmax activation function is used on the last dense layer which functions as the output layer. The architecture used for learning the fault location and type is depicted in Fig. 5.

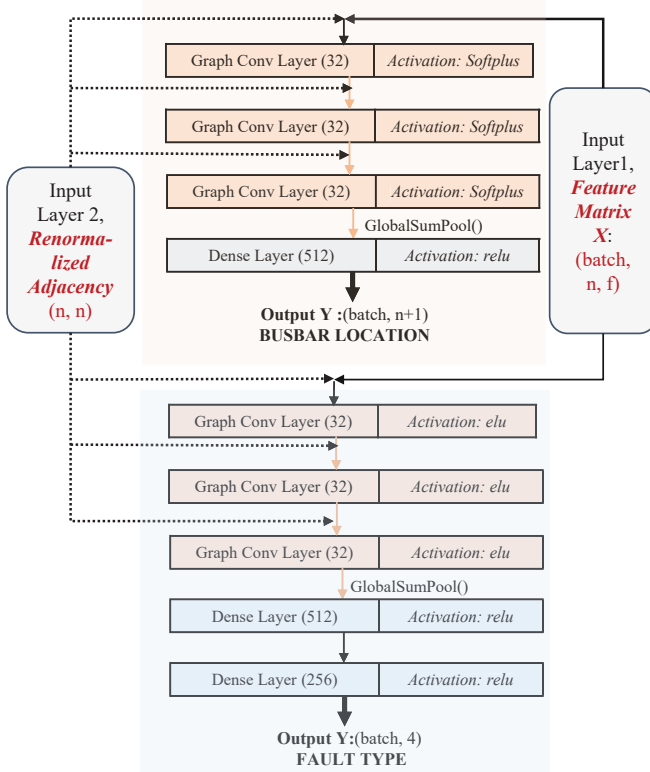


Fig. 5: Network architecture for learning the location and type of fault in SPS

C. Data preparation and preprocessing

The data for the graph learning framework is derived from the dynamic model of the SPS using the methodology described in Section II. The raw data comprises of voltage measurements at the various buses in the network corresponding to no fault and fault conditions.

A graph is constructed to represent the SPS, and its topology represented by the adjacency matrix remains unchanged for different data streams. Each data sample drawn from the simulation results consists of 3 phase voltage measurements at the 8 nodes of the test SPS. Hence, the feature matrix is represented as $X \in \mathbb{R}^{8 \times 3}$. The output of the learning model used for detecting the fault location is the busbar at which fault is initiated, Y . The no fault condition is also incorporated into Y wherein a value '0' represents no fault, '1' represents fault

at busbar 1 and so forth. The fault location for each data stream is converted into a one hot encoding which is represented as $Y \in \mathbb{R}^{1 \times 9}$. Similarly, in the case of the learning network used for classifying the type of fault, the output is encoded to represent the no fault condition and the three different kinds of faults. Thus, a value '0' indicates no fault, '1' indicates LG fault, '2' is used to denote LL fault, and '3' indicates 3L fault. The subsequent one hot encoding of output vector is represented as $Y \in \mathbb{R}^{1 \times 4}$.

The inputs, X and A , are preprocessed before passing onto the network model. The feature matrix is normalized such that attributes of the node falls within a sphere of radius 1 which is centered around the origin. The normalization of features corresponding to node k is expressed as:

$$\tilde{X}_k = \frac{X_k - \hat{X}}{\max(X)} \quad (8)$$

where \hat{X} is the centroid of the node attributes. The adjacency matrix is initially processed using (7). However, to avoid instability, it is renormalized as proposed in [14]. Therefore, (7) is modified to:

$$\tilde{A} = I + \hat{D}^{-\frac{1}{2}} \hat{A} \hat{D}^{-\frac{1}{2}} \quad (9)$$

where $\hat{A} = A + I$ and $\hat{D}_{ii} = \sum_{j=1}^n \hat{A}_{ij}$.

A total of 60,000 samples with fault at different buses and no fault are used by the model. The data distribution is represented in Fig. 6.

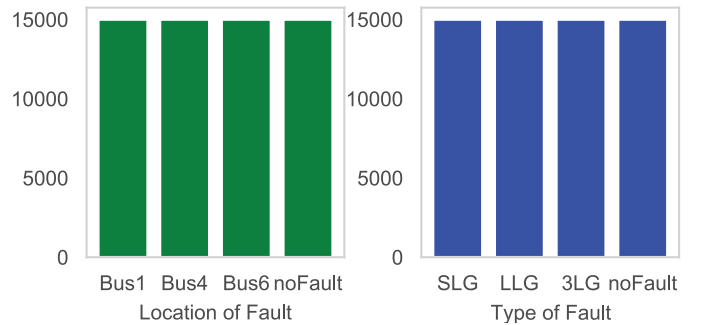


Fig. 6: Data distribution for learning location and type of fault

IV. RESULTS AND DISCUSSION

The shipboard power system is built on DigSILENT to perform dynamic simulations. The learning algorithm is implemented in Python using the Spektral library [25] with Tensorflow2 and Keras dependencies. In the model for learning both the fault location and fault type, a batch size of 32 is used for 1,000 epochs with an early stop patience of 200 epochs. The Adam optimizer which relies on a stochastic gradient descent technique based on adaptive estimation of first order and second order moments is used for learning the network parameters [26]. A learning rate of 0.001 is used along with the default values for other parameters associated with the Adam optimizer available in the tensorflow framework.

The adjacency matrix of the SPS which denotes its topology is extracted from the representative graph. It is further

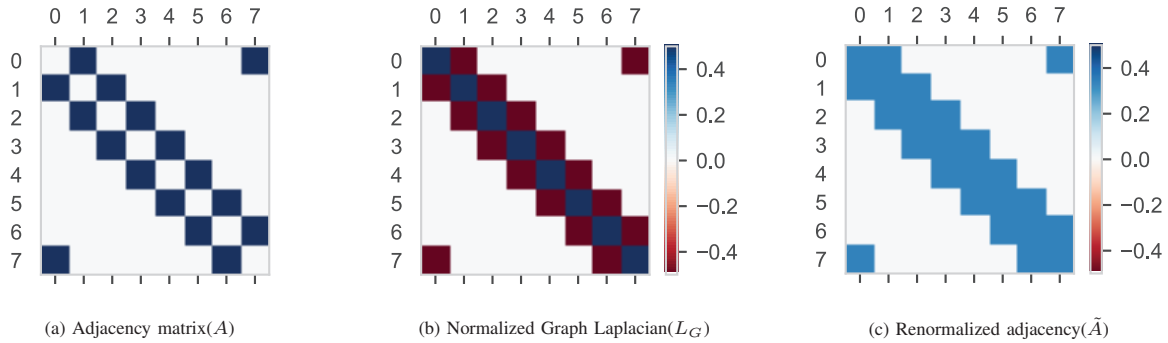


Fig. 7: Preprocessing the topology information of SPS network for GCN

processed as mentioned in Section III. The resulting adjacency matrix, the graph laplacian, and the adjacency matrix renormalized using (9) are illustrated in Fig. 7. As seen in the figure, the adjacency matrix is sparse and symmetric in nature. Also the corner entries depicted show the looped structure of SPS.

The performance of the learning algorithm is measured in terms of categorical accuracy and categorical cross entropy. These accuracy and loss metrics obtained during the test phase while detecting both the location and type of fault are presented in Table I. The performance of the graph learning model in detecting the fault location and fault type are shown in Fig. 8 and Fig. 9, respectively. Using an Intel Core i7-8565U 1.80GHz with 16 GB memory, the computation time taken to detect the fault location and fault type during the test phase is 2.80 ms and 3.25 ms, respectively.

TABLE I
PERFORMANCE OF LEARNING NETWORK DURING TEST PHASE

Network	Categorical Accuracy	Categorical Loss
Fault Location	99.38%	0.027
Fault Type	99.75%	0.015

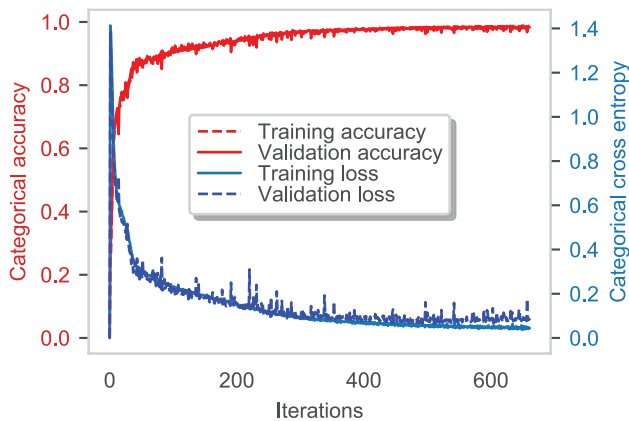


Fig. 8: Performance of learning network used for detecting fault location

A taxonomy table is presented in Table II to compare the proposed method in this work with published methods in the literature. Table II summarizes the fault detection,

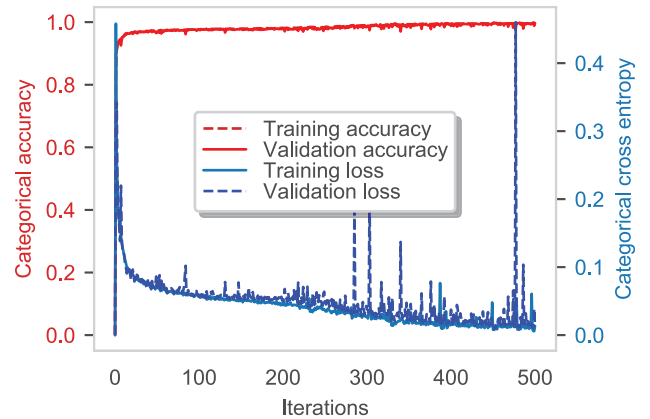


Fig. 9: Performance of learning network used for detecting fault type

classification, and location accuracies. It is important to note that the accuracies of other models reported here are directly taken from the references, which are not the fault detection accuracy on our 8-bus SPS model and are obtained from their specific networks.

TABLE II
THE ACCURACY OF DIFFERENT FAULT DETECTION MODELS

Model	Accuracy		
	Detection	Classification	Locating
Proposed GCN Model	99.75%	99.75%	99.38%
Decision Tree [27]	97%	85%	-
K-nearest neighbors [28]	90.4%	90.4%	-
Fully connected DNN [7]	-	95%	-
Fully connected DNN [9]	-	99.58%	-
Differential relay [27]	96%	-	-

V. CONCLUSION

In this paper, a GCN-based learning framework was developed for detecting the type and the location of the fault in a shipboard power network. The dynamic model of a shipboard power system was used to derive voltage measurements at various nodes in the network when a fault is initiated in the network. The measurements extracted along with the current topology of the network were fed into the learning module.

The GCN layers in the network architecture were used to capture both the spatial and spectral information encoded in the form of a featured graph. The latent representations of the data were learned by multiple GCN and fully connected layers. The developed model was found to detect the location and type of fault with more than 99% accuracy. Potential future direction of research involves performing fault diagnostics in a partially observable environment and investigating the performance of the algorithm in a dynamic network with varying topology.

ACKNOWLEDGMENT

This material is based upon work sponsored by the Department of the Navy, Office of Naval Research under ONR award number N00014-20-1-2795. Any opinions, findings, and conclusions or recommendations expressed in this material are those of the author(s) and do not necessarily reflect the views of the Office of Naval Research.

REFERENCES

- [1] R. R. B. Powers, "Automation as a manpower reduction strategy in navy ships," Ph.D. dissertation, Massachusetts Institute of Technology, 2016. [Online]. Available: <https://dspace.mit.edu/handle/1721.1/104386>
- [2] "Department of the Navy Unmanned campaign framework," Available at <https://www.navy.mil/Portals/1/Strategic>, 2021/03/16.
- [3] K. Satpathi, A. Ukil, and J. Pou, "Short-circuit fault management in dc electric ship propulsion system: Protection requirements, review of existing technologies and future research trends," *IEEE Transactions on Transportation Electrification*, vol. 4, no. 1, pp. 272–291, 2018.
- [4] J. J. Q. Yu, Y. Hou, A. Y. S. Lam, and V. O. K. Li, "Intelligent fault detection scheme for microgrids with wavelet-based deep neural networks," *IEEE Transactions on Smart Grid*, vol. 10, no. 2, pp. 1694–1703, 2019.
- [5] G. L. Kusic, "State estimation and fast fault detection for ship electrical systems," in *2007 IEEE Electric Ship Technologies Symposium*, 2007, pp. 209–214.
- [6] H. Livani and C. Y. Evrenosoğlu, "A fault classification method in power systems using dwt and svm classifier," in *PES TD 2012*, 2012, pp. 1–5.
- [7] N. K. Chanda and Yong Fu, "Ann-based fault classification and location in mvdc shipboard power systems," in *2011 North American Power Symposium*, 2011, pp. 1–7.
- [8] Y. Ma, D. Oslebo, A. Maqsood, and K. Corzine, "Dc fault detection and pulsed load monitoring using wavelet transform-fed lstm autoencoders," *IEEE Journal of Emerging and Selected Topics in Power Electronics*, pp. 1–1, 2020.
- [9] W. Li, A. Monti, and F. Ponci, "Fault detection and classification in medium voltage dc shipboard power systems with wavelets and artificial neural networks," *IEEE Transactions on Instrumentation and Measurement*, vol. 63, no. 11, pp. 2651–2665, 2014.
- [10] Q. Liu, T. Liang, and V. Dinavahi, "Deep learning for hardware-based real-time fault detection and localization of all electric ship mvdc power system," *IEEE Open Journal of Industry Applications*, vol. 1, pp. 194–204, 2020.
- [11] Y. Ma, D. Oslebo, A. Maqsood, and K. Corzine, "Pulsed-power load monitoring for an all-electric ship: Utilizing the fourier transform data-driven deep learning approach," *IEEE Electrification Magazine*, vol. 9, no. 1, pp. 25–35, 2021.
- [12] M. Henaff, J. Bruna, and Y. LeCun, "Deep convolutional networks on graph-structured data," *arXiv preprint arXiv:1506.05163*, 2015.
- [13] M. Defferrard, X. Bresson, and P. Vandergheynst, "Convolutional neural networks on graphs with fast localized spectral filtering," *arXiv preprint arXiv:1606.09375*, 2016.
- [14] T. N. Kipf and M. Welling, "Semi-supervised classification with graph convolutional networks," *arXiv preprint arXiv:1609.02907*, 2016.
- [15] M. Niepert, M. Ahmed, and K. Kutzkov, "Learning convolutional neural networks for graphs," in *International conference on machine learning*. PMLR, 2016, pp. 2014–2023.
- [16] J. Atwood and D. Towsley, "Diffusion-convolutional neural networks," *arXiv preprint arXiv:1511.02136*, 2015.
- [17] J. Gilmer, S. S. Schoenholz, P. F. Riley, O. Vinyals, and G. E. Dahl, "Neural message passing for quantum chemistry," in *International Conference on Machine Learning*. PMLR, 2017, pp. 1263–1272.
- [18] B. Donon, R. Clément, B. Donnot, A. Marot, I. Guyon, and M. Schoenauer, "Neural networks for power flow: Graph neural solver," *Electric Power Systems Research*, vol. 189, p. 106547, 2020.
- [19] C. Kim, K. Kim, P. Balaprakash, and M. Anitescu, "Graph convolutional neural networks for optimal load shedding under line contingency," in *2019 IEEE Power & Energy Society General Meeting (PESGM)*. IEEE, 2019, pp. 1–5.
- [20] M. Yu, Z. Zhang, X. Li, J. Yu, J. Gao, Z. Liu, B. You, X. Zheng, and R. Yu, "Superposition graph neural network for offshore wind power prediction," *Future Generation Computer Systems*, vol. 113, pp. 145–157, 2020.
- [21] K. Chen, J. Hu, Y. Zhang, Z. Yu, and J. He, "Fault location in power distribution systems via deep graph convolutional networks," *IEEE Journal on Selected Areas in Communications*, vol. 38, no. 1, pp. 119–131, 2019.
- [22] F. Shariatzadeh, N. Kumar, and A. K. Srivastava, "Optimal control algorithms for reconfiguration of shipboard microgrid distribution system using intelligent techniques," *IEEE Transactions on Industry Applications*, vol. 53, no. 1, pp. 474–482, 2017.
- [23] S. Senemmar and J. Zhang, "Deep learning-based fault detection, classification, and locating in shipboard power systems," in *IEEE Electric Ship Technologies Symposium (ESTS)*, August 2021.
- [24] "PowerFactory - Digsilent," Mar 2021, [Online]; accessed 16. Mar. 2021]. [Online]. Available: <https://www.digsilent.de/en/powerfactory.html>
- [25] D. Grattarola and C. Alippi, "Graph neural networks in tensorflow and keras with spektral," *arXiv preprint arXiv:2006.12138*, 2020.
- [26] D. P. Kingma and J. Ba, "Adam: A method for stochastic optimization," *arXiv preprint arXiv:1412.6980*, 2014.
- [27] D. P. Mishra, S. R. Samantaray, and G. Joos, "A combined wavelet and data-mining based intelligent protection scheme for microgrid," *IEEE Transactions on Smart Grid*, vol. 7, no. 5, pp. 2295–2304, 2016.
- [28] T. S. Abdelgayed, W. G. Morsi, and T. S. Sidhu, "A new approach for fault classification in microgrids using optimal wavelet functions matching pursuit," *IEEE Transactions on Smart Grid*, vol. 9, no. 5, pp. 4838–4846, 2018.